Adhesion and friction in gecko toe attachment and detachment

Yu Tian*†, Noshir Pesika*, Hongbo Zeng*, Kenny Rosenberg*, Boxin Zhao*, Patricia McGuiggan*, Kellar Autumn‡, and Jacob Israelachvili*§

*Department of Chemical Engineering and California NanoSystems Institute (CNSI), University of California, Santa Barbara, CA 93106; †State Key Lab of Tribology, Department of Precision Instruments, Tsinghua University, Beijing 100084, People's Republic of China; and ‡Department of Biology, Lewis and Clark College, Portland, OR 97219

Contributed by Jacob Israelachvili, October 5, 2006 (sent for review August 4, 2006)

Geckos can run rapidly on walls and ceilings, requiring high friction forces (on walls) and adhesion forces (on ceilings), with typical step intervals of ≈20 ms. The rapid switching between gecko foot attachment and detachment is analyzed theoretically based on a tape model that incorporates the adhesion and friction forces originating from the van der Waals forces between the submicron-sized spatulae and the substrate, which are controlled by the (macroscopic) actions of the gecko toes. The pulling force of a spatula along its shaft with an angle θ between 0 and 90° to the substrate, has a ''normal adhesion force'' contribution, produced at the spatula-substrate bifurcation zone, and a ''lateral friction force'' contribution from the part of spatula still in contact with the substrate. High net friction and adhesion forces on the whole gecko are obtained by rolling down and gripping the toes inward to realize small pulling angles θ between the large number of spatulae in contact with the substrate. To detach, the high adhesion/friction is rapidly reduced to a very low value by rolling the toes upward and backward, which, mediated by the lever function of the setal shaft, peels the spatulae off perpendicularly from the substrates. By these mechanisms, both the adhesion and friction forces of geckos can be changed over three orders of magnitude, allowing for the swift attachment and detachment during gecko motion. The results have obvious implications for the fabrication of dry adhesives and robotic systems inspired by the gecko's locomotion mechanism.

tape model | pulling angle | lever function | spatula | seta

The extraordinary climbing ability of geckos is considered a remarkable design of nature that is attributed to the fine structure of its toes, which contain setal arrays consisting of hundreds of spatulae on each seta. These fine structures allow for intimate contact between the spatulae and surfaces to obtain high adhesion and friction forces on almost any surface, whether hydrophilic or hydrophobic, rough or smooth, through weak van der Waals forces (1–4). The focus of studies (4–26) has been to understand the friction and adhesion of geckos with a goal to potentially fabricate dry ''responsive'' adhesives.

The macro-, meso-, micro-, and nanoscale structures that make up the hierarchical structure of the gecko toe pads have been imaged by different microscopy techniques (5). The whole hierarchical structure of a Tokay gecko is shown in Fig. 1 *a–f*: one body with four feet, each foot with five toes, each toe with ≈20 rows of sticky lamellae, each lamella with many setal arrays consisting of thousands of setae, which amounts to ≈200,000 setae per toe, and each seta consisting of hundreds to 1,000 spatulae at its end.

The corresponding forces achieved by the different hierarchical structures are shown in the right of Fig. 1 *g–i*. The lateral friction force F_L and normal adhesion force F_n resulting from each spatula (Fig. 1*i*) must be vectorially summed over all the spatulae to obtain the net (normal and lateral) force F_{tot} acting on the entire body of the gecko (Fig. 1*g*). Because the toes on each foot, and the feet themselves, all point in different directions, the summation of $F(\theta) = [F_n \sin\theta + F_L \cos\theta]$ over all angles θ is not a trivial matter, and neither is the calculation (and measurement) of the normal and lateral forces F_n and F_L, which are not constant but also θ-dependent. The above equation does show, however, that both the (local) adhesion and friction forces together determine the net or total force F_{tot}.

The hierarchical structures with large dimensions, i.e., the feet, toes, lamella, and setal arrays, are relatively easy to approach. The kinetics of gecko motion using the friction forces of their feet have been reported recently (27, 28). The tested friction force of two front feet is ≈20.1 N (6). The ''frictional adhesion'' of a setal array on a glass surface has also been tested recently (7). In contrast, it is hard to study the mechanics of a single seta or a single spatula due to their small dimensions. The limited data on setae or spatulae are as follows. First, the maximum friction force of a single seta (with 100–1,000 spatulae) is ≈200 μN, and the adhesive force is 20–40 μN (2, 8). A model of the seta as a cantilever beam has been proposed that agrees with the measurements on setal arrays (9). Second, Huber and colleagues (10, 20) glued a seta perpendicular to the end of an atomic force microscope cantilever beam. With only a few spatulae on the end of the setal shaft, they measured the adhesion force of a single spatula to be ≈10 nN. Sun *et al.* (11) measured the adhesion force between the spatulae and a hydrophobic silicon cantilever of 2–7 nN, and 6–16 nN for a hydrophilic silicon cantilever. From the above experiments, it is apparent that the friction forces are much higher than the adhesion forces, which is one of the main issues we analyze in this paper.

Also, the effect of surface roughness on the adhesion of elastic plates has been discussed theoretically (12, 13); however, the experimental data are limited. In particular, the separate contributions of the normal adhesion and lateral friction forces have not been fully investigated. Most importantly, the rapid switching on and off of the strong adhesion and friction forces during a step (involving attachment followed by detachment) is still an open issue.

Artificial dry adhesive surfaces mimicking geckos have been fabricated by using polymer pillar structures (9, 14, 15). The resulting structures agree with theoretical studies showing that the shapes of the structures play a minimal role on the adhesion force, whereas the size and density of the structures play important roles, especially when the lateral dimensions falls below 100 nm (16, 17). However, a seta is not a simple cantilever and the spatulae on its end are not simple pillars or fibers. The release of a single seta has been found to occur at a characteristic

Author contributions: J.I. designed research; Y.T., N.P., and H.Z. performed research; K.A. contributed new reagents/analytic tools; Y.T., N.P., H.Z., K.R., B.Z., and P.M. analyzed data; and Y.T. wrote the paper.

The authors declare no conflict of interest.

§To whom correspondence should be addressed. E-mail: jacob@engineering.ucsb.edu

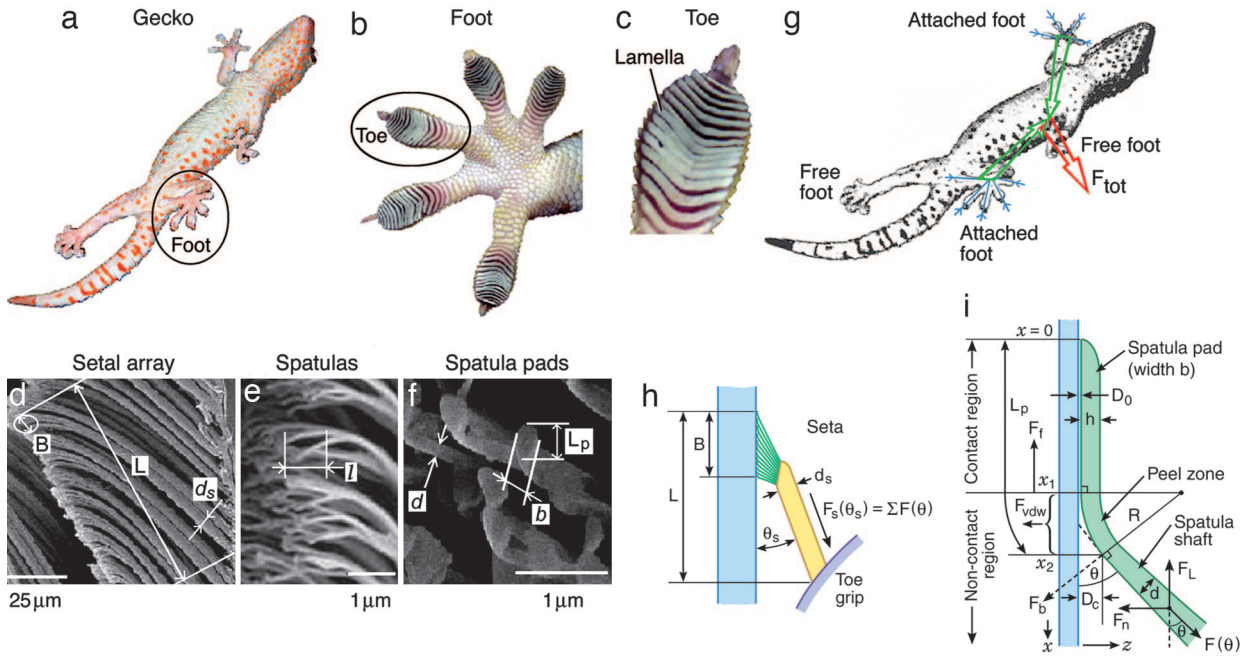

Fig. 1. The hierarchical structures of geckos. (*a–f*) Structures shown in the order of decreasing size. (*g–i*) The various forces and other parameters used in the equations of this paper. The angles θ are often small (<45°) (7, 8), which makes the friction force contributions nonnegligible in the forces associated with gecko biomechanics.

angle θ_s of ≈30° (8) indicating that geometry plays an important role in the detachment of a seta.

Because the thin tape-like spatula pads are ultimate structures in contact with the substrate, they might be expected to be the most important in determining the adhesion and friction of geckos. Therefore, it is reasonable to start with a consideration of the forces acting on these, the smallest structures in the hierarchy (Fig. 1 *d–f*). A few studies (13, 17, 20, 21) of the peeling of a single spatula have been analyzed in terms of the Kendall peeling model as

$$(F/b)^2/2hE + (F/b)(1 - \cos\,\theta) - G = 0, \qquad [1]$$

where F is the peeling force [$=F(\theta)$ in Fig. 1], b is the width of the tape, h is the thickness of the tape, E is the elastic modulus of the tape, θ is the peeling angle, and G is the "crack energy" required to fracture a unit area of interface at a peeling angle of $\theta = 90°$. However, the kind of force and how this force contributes to the crack energy G have not been clarified, and no friction forces are considered in the Kendall model. A satisfactory peeling model for adhesive tape is yet to be developed (22), and the few simple models that do exist are not suitable for analyzing the pulling of gecko spatulae.

In this work, we theoretically analyze the adhesion and friction mechanisms in gecko attachment and detachment based on a model that includes both the adhesion and friction forces between a single spatula and a substrate. Although we have based our analysis on the assumption that the forces are of van der Waals origin, we find, as discussed later, that our results are quite general and should be valid for other types of short-range noncovalent interaction forces. The mechanism at the spatula and seta levels (nano- to micrometer scales) is seen to be intimately coupled to and coordinated with the actuations of the larger structures in the hierarchy: the toes, feet, and bodies of geckos. Our theoretical considerations are also based on recent experimental studies and observations (2, 8, 10, 11, 17–19), including results from our laboratory (P.N., Y.T., B.Z., H.Z., K.R., P.M., K.A., and J.I., unpublished data). The implications for the design of dry adhesive surfaces that can reliably and efficiently adhere to, and easily release from, any surface are suggested.

Geometric Parameters of Setae and Spatulae

The final two levels of the hierarchical structures of geckos are the seta and their spatulae. A seta has a length of approximately $l_s = 120$ μm, a cross-sectional diameter $d_s = 4.2$ μm (Fig. 1*d*). It branches into hundreds of spatulae through several shaft levels. The final shaft level, i.e., the spatula shaft, has a diameter of approximately $d = 0.1$ μm and a length of $l = 0.8$ μm. A spatula pad held at the end of a spatula shaft (Fig. 1 *e* and *f*) has approximate dimensions of 0.3 μm (length, L_p) × 0.2 μm (width, b) × 5 nm (thickness, h). The bending inertia of the seta shaft, spatula shaft and spatula pads are $I_s = 1.5 \times 10^{-23}$ m^4, $I' = 4.9 \times 10^{-30}$ m^4, and $I = 1.7 \times 10^{-32}$ m^4, respectively. The bulk elastic modulus E of the β keratin-like protein that constitutes the seta is $E = 2.6$ GPa (26) but may change for different animals and different animal structures. In this analysis we will take $E = 2$ GPa.

Adhesion and Friction of a Single Spatula

Origin of Friction and Adhesion Between Two Planar Surfaces. It is worth considering the molecular origin of the friction and adhesion forces from the van der Waals forces between the two surfaces (29–32). As shown in Fig. 2*a*, for two contacting planar surfaces, the surface potential E_x along the x direction (parallel to the surfaces) can be described approximately by a sinusoidal function (although any amplitude-varying function that maps the surface potential landscape will do)

$$E_x = E_0 \sin(2\pi x/x_0), \qquad [2]$$

so that the friction force (Fig. 2*a Lower*) is

$$F_f = -dE_x/dx = -(2\pi E_0/x_0)\cos(2\pi x/x_0), \qquad [3]$$

where x_0 is a critical spacing related to the atomic lattice, molecular or asperity dimension on the spatula and substrate

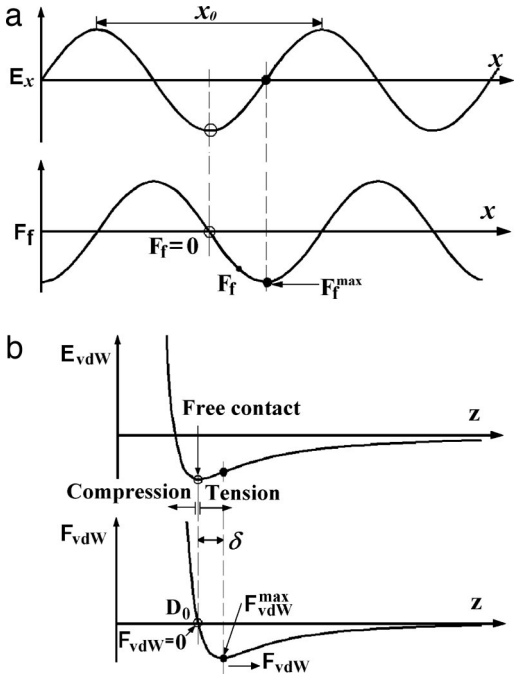

Fig. 2. The interaction between two surfaces. (*a*) The origin of the lateral friction force F_f or F_L from a consideration of the periodic surface interaction potential along the *x* direction. The period may be a lattice dimension or mean distance between asperities (31), and the forces themselves may be due to van der Waals or some other interactions. (*b*) The surface–surface potential in the normal (*z* direction) to the substrate, which determines the normal attractive or adhesion force, F_n or F_{vdW}. In each case, there is a maximum or critical force which, when exceeded, the surfaces move, either laterally (frictional sliding when $F_f = F_f^{max}$) or normally (detachment when $F_{vdW} = F_{vdW}^{max}$).

surfaces. When $E_x = 0$, $F_L = F_f^{max}$, the maximum static friction force that can be obtained from two contacting adhering surfaces (in the absence of an external load); at this lateral force or above, the surfaces begin to slide or slip. If the applied external force along the x direction is $F_L \leq F_f^{max}$, the friction force is simply $F_f = F_L$, and the surfaces remain stuck (although there may be some slow creep). In this work, we show that $F_L \leq F_f^{max}$ is usually satisfied during gecko attachment and detachment, i.e., that the lateral force never reaches the "critical" point where there is slip, although there may be some creep.

As shown in Fig. 2*b*, the normal potential E_z and the normal force F_{vdW} between two surfaces along the z direction can be described by a Lennard–Jones-type potential involving an attractive energy E_A and a repulsive energy E_R as

$$E_z = -E_A(z/z_0)^{-n} + E_R(z/z_0)^{-m} \quad (m > n), \qquad [4]$$

$$F_{vdW} = -dE_z/dz = -(nE_A/z_0)\,(z/z_0)^{-(n+1)} + (mE_R/z_0)\,(z/z_0)^{-(m+1)}. \qquad [5]$$

When E_z is at its minimum (equilibrium) value, it corresponds to $F_{vdW} = 0$ with a surface gap distance D_0. When two surfaces are pressed together with $D < D_0$, the force F_{vdW} is repulsive. When two surfaces are at $D > D_0$, F_{vdW} is attractive, reaching a maximum value of $F_n = F_{vdW}^{max}$ (the "adhesion" or "pull-off" force), at which point the surfaces spontaneously detach. The force between the two surfaces integrated from $D = D_0$ to $D = \infty$ is also net attractive, and may also be considered as an adhesion force. Because the repulsive component in Eqs. **4** and **5** is usually very steep, it may be approximated as a hard wall for $D < D_0$, whereas for two flat surfaces, the maximum attractive force per unit area is (29)

$$P_{vdW}^{max} \approx A/6\pi D_0^3, \qquad [6]$$

where A is the Hamaker constant. However, at larger gap distances $D > D_0$, the van der Waals force or pressure between two flat surfaces is

$$P_{vdW} = A/6\pi D^3. \qquad [7]$$

Force Balances in Pulling a Spatula. As shown in Fig. 1*i*, there are three force regimes: (*i*) a contact region from $x = 0$ to $x = x_1$ where the attractive van der Waals force is balanced by the repulsive steric surface force (the second term in Eqs. **4** and **5**), and where the total force on the spatula is therefore zero; (*ii*) a transition "peel zone" between x_1 and x_2 where the integrated van der Waals force F_{vdW} of the spatula is balanced by the force $F(\theta)$ along the spatula shaft; and (*iii*) for $x > x_2$, the van der Waals force acting on the shaft is too weak and is negligible, so the tension or pulling force remains constant and equal to $F(\theta)$ along the shaft. $F(\theta)$ can be written as

$$F(\theta) = F_n \sin\theta + F_L \cos\theta, \qquad [8]$$

where the normal and lateral components F_n and F_L are defined in Fig. 1*i*. Ignoring the small bending force $F_b(\theta - 90°)$ of the spatula because of its low bending inertia I (which contributes to both F_n and F_L; see supporting information, which is published on the PNAS web site), these components can be written as

$$F_n = F_{vdW} = F(\theta)\sin\theta, \qquad [9]$$

and

$$F_L = F_f = F(\theta)\cos\theta. \qquad [10]$$

Geometry of a Pulled Spatula. Applying Eq. **7**, F_{vdW} at the spatula peel zone is obtained by integrating Eq. **7** along the length between x_1 and x_2 of radius R (Fig. 1*i*). Point x_1 is the last contact point between the spatula and the substrate. Point x_2 is the point beyond which the van der Waals force can be neglected (and the spatula is no longer curved), which occurs at a (critical) separation distance D_c. We take D_c to be 1 nm, being five times the contact separation of $D_0 \approx 0.3$ nm. The van der Waals force varies as $1/D^3$, so at $D(x_2) = D_c$ the force is <1% of the value just outside the contact at $x \geq x_1$. The radius of the spatula R is related to D_c and θ by

$$R = D_c/(1 - \cos\theta). \qquad [11]$$

However, Eq. **11** must break down for large θ values (small R) because it predicts radii that are smaller than the thickness of the spatula, h. For example, for $D_c = 1$ nm, $\theta = 90°$ corresponds to $R = 1$ nm, which is impossible since $h \approx 5$ nm. We shall assume that the smallest possible (limiting) radius is $R = 10$ nm (twice the spatula thickness), which occurs when $\theta \geq 90°$. However, for small θ, the curvature should be close to that given by Eq. **11** with $D_c = 1$ nm; for example, $R = 1{,}640$ nm for $\theta = 2°$. To obtain a physically realistic functional form for R in terms of θ that is valid at all angles, we fitted the above two limits (Eq. **11** for small θ and $R = 10$ nm as $\theta \to 90°$) using an empirical power law of the form

$$R = 4{,}215 \times \theta^{-n}, \qquad [12]$$

where $n = 1.35$, R is in nm, θ is in degrees and only valid between 0 and 90°. Eq. **12** satisfies both limits and has approximately the right shape in between, as shown in Fig. 3 (middle curve). The length of the spatula at the peel zone from x_1 to x_2 is then

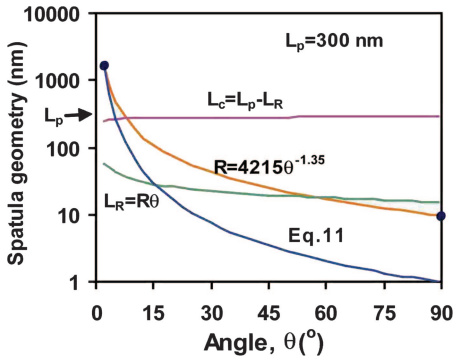

Fig. 3. Geometric parameters of a spatula when pulled at different angles.

$$L_R = R\theta, \qquad [13]$$

whereas the length in contact with the surface (from $x = 0$ to x_1) is

$$L_c = x_1 = L_p - L_R. \qquad [14]$$

where, typically, $L_p = 300$ nm. L_R is shown in Fig. 3 (lower curve) where it is found to be 5–20% of L_p when $\theta \geq 2°$; and L_c is also shown, where it is found to be close to L_p for all values of θ above 2°.

Adhesion of a Pulled Spatula. Based on the geometric relations shown in Figs. 1*i* and 3, the attractive force in the peel zone F_{vdW} can be obtained by integrating the vdW force, Eq. **7**, from $\phi = 0$ to $\phi = \theta$ follows

$$F_{vdW} = \int_0^\theta (A/6\pi D^3)\cdot bRd\phi$$

$$= \int_0^\theta \{A/6\pi[D_0 + R(1-\cos\phi)]^3\}\cdot bRd\phi. \qquad [15]$$

Alternatively, a rough estimate of F_{vdW} can be obtained from the standard expression for the force between half a cylinder of radius R and a flat surface (23)

$$F_{vdW} = AbR^{1/2}/16\sqrt{2}D^{5/2}. \qquad [16]$$

Fig. 4 shows $F_{vdW}(\theta)$, normalized by $F_{vdW}(90°)$, as predicted by Eqs. **15** and **16**. We see that the two equations give almost the same ratio. Taking the R values defined in Fig. 3, $b = 0.2$ μm,

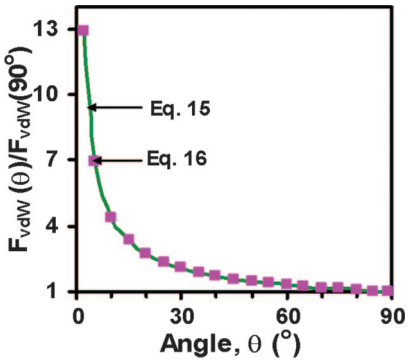

Fig. 4. The normalized adhesion force at different pulling angles, θ, as determined by Eqs. **15** and **16**.

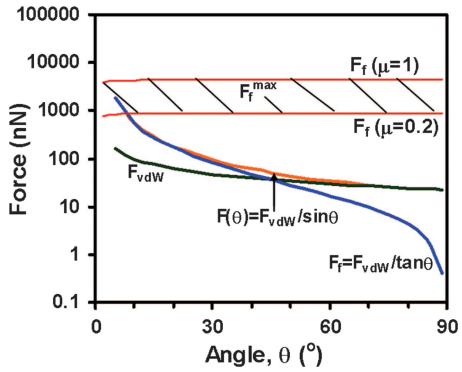

Fig. 5. The absolute values of the normal (adhesion) force component F_{vdW}, the lateral (friction) force component F_f, the net pulling force $F(\theta)$, and the maximum friction force F_f^{max} that can be obtained from a spatula pad in contact with a substrate (shaded band).

and $A = 0.4 \times 10^{-19}$ J as before, the absolute values of F_{vdW} vs. θ are shown by the curve F_{vdW} in Fig. 5, which ranges from ≈20 (at 90°) to 150 nN (at 5°). We note that this uses estimates for the values of A, b, D_c, and D_o to calculate the F_{vdW}. Larger values of the F_{vdW} could be obtained by using larger values for A, b, D_c, or a smaller value for D_o.

Available Maximum Friction Force of a Pulled Spatula. We can use Eq. **6** to estimate the attractive component $F_{c,vdW}$ in the "contact region" ($x < x_1$ in Fig. 1), which determines the adhesion force contribution to the friction force, F_f. Taking $A = 0.4 \times 10^{-19}$ J, and $D_0 = 0.3$ nm for the surface–surface separation of two contacting surfaces (23), Eq. **6** gives $P_{c,vdW} = 80$ MPa. The net attractive force in the contact region is, therefore,

$$F_{c,vdW} = L_c \times b \times P_{c,vdW}, \qquad [17]$$

where $L_c \times b$ is the contact area of a spatula with the substrate. We can now estimate the maximum friction force using the general equation for "adhesion-controlled" friction based on the definition of the friction coefficient in ref. 30

$$F_f^{max} = \mu F_{c,vdW}, \qquad [18]$$

where μ is the friction coefficient. Because μ for a polymer material rubbing against a van der Waals (chemically inert) surface usually ranges from 0.2 to 1.0 (32), F_f^{max} is predicted to be ≈900–4,500 nN as shown in Fig. 5. The friction force of a single spatula has never been measured directly. Autumn *et al.* (8) carried out a friction test on a single seta obtaining a maximum friction force of ≈200 μN. Taking the number of spatulae on a single seta to be 100–1,000, then F_f^{max} of a single spatula is 200–2,000 nN, which is in agreement with the above theoretical estimate.

Obtained Friction Force of a Pulled Spatula. According to Eqs. **8–10**, the friction force is $F_f = F_{vdW}/\tan\theta$, and the total pulling force is $F(\theta) = F_{vdW}/\sin\theta$. These two curves are shown in Fig. 5. Fig. 5 also shows the range of maximum possible values for $F(\theta)$ before the surfaces detach or slip. This regime, shown by the horizontal shaded band is determined mainly by F_f^{max}, as previously shown. The condition $F(\theta) < F_f^{max}$ is clearly satisfied for angles θ greater than ≈10°. Fig. 5 also shows that the pulling force $F(\theta)$ can vary by more than two orders of magnitude depending on θ and that for small θ ($\theta < 30°$) it is determined mainly by the friction force while for large θ ($\theta > 60°$) it is determined mainly by the adhesion force, the cross-over angle

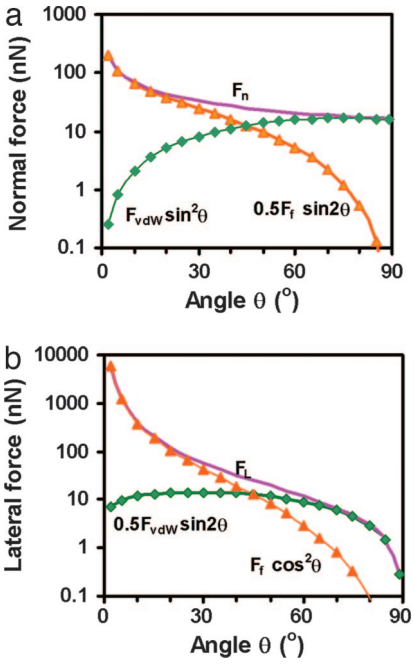

Fig. 6. Total normal adhesion force $F_n(\theta)$ (*a*) and total lateral force $F_L(\theta)$ (*b*) of a single spatula, and the contributions from F_{vdW} and F_f to the them as given by Eqs. **19** and **20**. Note that, according to Eqs. **9** and **10**, $F_f = F_{vdW}/\tan\theta$.

being at ≈40°. When $F(\theta) > F_f^{max}$ at very small angles, the spatula will slide or slip on the substrate.

Comparison with Experimental Results of Adhesion of a Single Spatula. Due to the uncertainty of A between spatulae and different substrates, it is hard to theoretically predict an accurate value for F_{vdW} of a single spatula. Taking the maximum experimental friction force of a single seta of 200 μN (8) as corresponding to a low pulling angle of, say, 10°, and assuming 500 spatulae per seta, we have $F_f(10°) = 400$ nN (compare the previous estimate in the range 200–2,000 nN above). The calculated $F_{vdW}(10°) = F_f(10°) \times \tan(10°) = 70$ nN per spatula is within the range reported for the adhesive force of a single seta (2, 8). This value corresponds to $F_{vdW}(90°) = 16$ nN for a single spatula, close to the values of 10 nN reported by Huber *et al.* (10), and 2–16 nN reported by Sun *et al.* (11) in which the spatulae were pulled off at ≈90°. However, the existing data of spatula adhesion forces have never been done at controlled angles θ; thus, it is reasonable that the measured values have a distribution within the range of our estimates of F_n. Further experiments on the adhesion forces of single spatulae under controlled pulling angles should be done to directly obtain the dependence of F_n on θ.

Friction Contribution to Normal and Lateral Pulling Forces, F_n and F_L. As already noted, one cannot get a high normal (adhesion) force F_n at small pulling angles unless the lateral (friction) force is high. According to Eqs. **8–10**, the total normal (measured adhesion) force is

$$\begin{aligned} F_n(\theta) &= F(\theta)\ \sin\theta \\ &= (F_f\cos\theta + F_{vdW}\sin\theta)\ \sin\theta \\ &= 0.5F_f\sin 2\theta + F_{vdW}\sin^2\theta. \end{aligned} \qquad [19]$$

The contributions of F_{vdW} and F_f to F_n are shown in Fig. 6 *a* using the above estimate of $F_{vdW}(10°) = 70$ nN. $F_n(\theta)$ is mainly contributed by F_{vdW} at high θ (>60°) and by F_f at a small θ (<30°), but the highest adhesion force is obtained at small θ due to the high resolved friction force. This is important for understanding how geckos get their high adhesion force, enabling them to cling to ceilings. Fig. 6 *a* also demonstrates the interplay between the angle-resolved values of F_{vdW} and F_f.

Similarly, we can obtain the F_{vdW} and F_f contributions to the total lateral pulling force F_L as

$$\begin{aligned} F_L(\theta) &= F(\theta)\ \cos\theta \\ &= (F_f\cos\theta + F_{vdW}\sin\theta)\ \cos\theta \\ &= F_f\cos^2\theta + 0.5F_{vdW}\sin 2\theta, \end{aligned} \qquad [20]$$

which are plotted in Fig. 6*b*. As might be expected, the lateral force is dominated by the friction force for angles θ below 45°, and can reach very high values as $\theta \to 0$. This is important for understanding how geckos get their high friction force, enabling them to cling to walls.

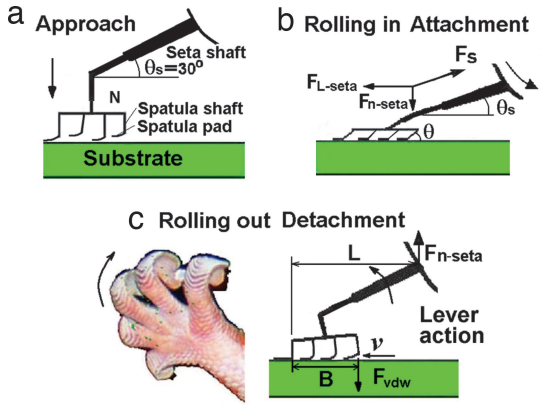

Fig. 7. Sketches of attachment and detachment of a single seta by (*a*) approaching the substrate rolling (or gripping) in (*b*) and rolling (or peeling) out (*c*) the toes. The image in *c Left* is from the left back foot in Fig. 1*a*.

Adhesion and Friction of a Seta

Seta Attachment. As shown in Fig. 1 *d–f* and sketched in Fig. 7*a*, in their natural configuration, the spatula pads are at an angle of ≈30° to the seta shaft, and are approximately normal to the spatula shafts. Therefore, when the spatula pads adhere to the substrate in a near-parallel configuration (Fig. 7*a*), the angle of the spatula shafts to the substrate will be close to 90°, corresponding to a weak adhesion force of about $NF_{vdW}(90°) = 8$ μN [taking the number of spatulae in contact with the substrate as $N = 500$, and $F_{vdW}(90°) = 16$ nN].

When geckos roll in and grip their toes inward (27) as sketched in Fig. 7*b*, the pulling angle θ_s of the seta shaft to the substrate will range from 0 to 30°, whereas the pulling angles θ of the spatula shafts to the substrate will range from 0 to 90°. The normal and lateral pulling force, $F_{n\text{-seta}}$ and $F_{L\text{-seta}}$, at the end of the seta shaft should satisfy $F_{L\text{-seta}} = F_{n\text{-seta}}/\tan\theta_s$. A tighter gripping (pulling in) of the toes leads to a smaller θ and θ_s, and to a larger number of spatulae in contact with the substrate. This results in both a higher friction and adhesion at the seta shaft. Thus, taking $N = 500$, $F_{vdW}(10°) = 70$ nN, and assuming $\theta = \theta_s = 10°$, then $F_{n\text{-seta}} = NF_{vdW}(10°) = 35$ μN, and $F_{L\text{-seta}} = F_{n\text{-seta}}/\tan 10° = 200$ μN, compared to the weak adhesion force of ≈8 μN for $\theta = 90°$ and $\theta_s = 30°$. This may be the microscopic explanation for why the gripping or pulling in action is important for geckos to obtain high friction and adhesion, as found in recent experiments (7, 8, 26–28), and it may also explain why geckos tend to spend more time on walls than on ceilings.

Seta Detachment. During the rolling out of toes to detach from a substrate, the setae are relaxed back to their initial free (natural) state with $\theta_s \approx 30°$ and $\theta \approx 90°$ when the toes cross over from a rolling-in to a rolling-out process (Fig. 7 *b* and *c*). If rolling continues as shown in Fig. 7*c*, then the spatulae will come off in sequence from right to left. Taking $N' = 20$ as the average number of spatulae detaching at any instant time per seta, v the peeling speed along the spatula bundle width B, $T = B/v$ as the peeling time of a single seta, then the average normal releasing force is

$$F_{\text{n-seta}} = \frac{1}{T}\int_{t=0}^{t=T} N'F_{\text{vdW}} \times (B - vt)/L\,dt$$

$$= N'F_{\text{vdW}} \times B/2L. \quad \textbf{[21]}$$

Eq. **23** can also be thought of the detachment force of $N'F_{\text{vdW}}$ being reduced by the lever action of the seta shaft by a factor of $B/2L$, where L is the seta shaft projection on the substrate, $B/2$ is the distance to the middle point of the contact region. Taking $F_{\text{vdW}} \cong F_{\text{vdW}}(90°) = 16$ nN, $B = 10$ μm and $L = 100$ μm, as estimated from Fig. 1, the normal releasing force of a single seta is $F_{\text{n-seta}} = 32$ nN, which is one-thousandth of $F_{\text{n-seta}}(10°) = 35$ μN in attachment. The typical detachment angle of a single seta θ_s, independent of the applied detachment force, was found to be $\approx 30°$ (8), which is close to its natural state. This result is consistent with the above mechanism in which a seta releases easily in this state.

The mechanisms of geckos switching rapidly between high friction and adhesion forces in attachment to a very low adhesion force in detachment were explored based on the van der Waals interactions between the spatulae and the substrate surface, rather than former derivations based on existing contact or peeling models (9, 18, 19). Our model is based on a force rather than energy balance, and is fully analytic rather than numerical or qualitative. The model also considers the role of the specific geometries of the hierarchical structures involved, includes both the adhesion and friction forces, and covers both attachment and detachment (the latter via a "lever" mechanism). Although given the assumption of our model, the conclusion should apply to other types of short-range noncovalent surface forces. High friction and adhesion forces are obtained by rolling down and gripping in the toes tightly to attain small pulling angles of the spatulae on the substrate (7). To detach, a very small release force is obtained by releasing the grip and rolling (peeling) the toes outward to detach the spatulae perpendicularly from the substrate helped by the lever action of the seta shaft.

Our analysis leads us to the conclusion that both the lateral friction force and normal adhesion force of a single seta can be changed by more than three orders of magnitude. This range should also apply to the whole gecko foot. For different motions, on level ground, vertical wall, or ceiling, geckos can control their feet and toes at different positions, angles, and stresses to acquire the desired friction and adhesion forces (7).

The switching of gecko toes between attachment and detachment, utilization of the nanotape-like functions of the spatula pads, the orienting actions of the seta shaft, could be incorporated in the fabrication of dry adhesive surfaces and robotics, rather than just using simple pillar-like structures without considering the mechanisms of attachment and detachment, and the manipulation of the normal and lateral surface forces by the toes and feet.

This work was sponsored by Institute for Collaborative Biotechnologies Grant DAAD19-03-D-0004 from the U.S. Army Research Office and Director of Central Intelligence/National Geospatial Intelligence Agency Grant HM1582-05-2022. B.Z. was supported by a Natural Sciences and Engineering Research Council of Canada postdoctoral fellowship award, and Y.T. thanks Tsinghua University for a Huaxin Distinguished Scientist Scholarship.

1. Russell AP (1975) *J Zool (London)* 176:437–476.
2. Autumn K, Sitti M, Peattie A, Hansen W, Sponberg S, Liang YA, Kenny T, Fearing R, Israelachvili J, Full RJ (2002) *Proc Natl Acad Sci USA* 99:12252–12256.
3. Ruibal R, Ernst V (1965) *J Morphol* 117:271–294.
4. Hiller U (1975) *J Bombay Nat Hist Soc* 73:278–282.
5. Russell AP, Bauer AM, Laroiya R (1997) *J Zool (London)* 241:767–790.
6. Irschick DJ, Austin CC, Petren K, Fisher R, Losos JB, Ellers O (1996) *Biol J Linn Soc* 59:21–35.
7. Autumn K, Dittmore A, Santos D, Spenko M, Cutkosky M (2006) *J Exp Biol*, in press.
8. Autumn K, Liang YA, Hsieh ST, Zesch W, Chan WP, Kenny WT, Fearing R, Full RJ (2000) *Nature* 405:681–685.
9. Autumn K, Majidi C, Groff R, Dittmore A, Fearing R (2006) *J Exp Biol*, in press.
10. Huber G, Mantz H, Spolenak R, Mecke K, Jacobs K, Gorb SN, Arzt E (2005) *Proc Natl Acad Sci USA* 102:16293–16296.
11. Sun W, Neuzil P, Kustandi TS, Oh S, Samper VD (2005) *Biophys J* 89:L14–L17.
12. Persson BNJ (2003) *J Chem Phys* 118:7614–7621.
13. Persson BNJ, Gorb S (2003) *J Chem Phys* 119:11437–11444.
14. Geim AK, Dubonos SV, Grigorieva IV, Novoselov KS, Zhukov AA (2003) *Nat Mater* 2:461–463.
15. Majidi C, Groff R, Autumn K, Baek S, Bush B, Gravish N, Maboudian R, Maeno Y, Schubert B, Wilkinson M, *et al.* (2006) *Phys Rev Lett*, in press.
16. Gao H, Yao H (2004) *Proc Natl Acad Sci USA* 101:7851–7856.
17. Spolenak R, Gorb S, Gao HJ, Arzt E (2004) *Proc R Soc London Ser A* 461:305–319.
18. Autumn K, Hsieh ST, Dudek DM, Chen J, Chitaphan C, Full RJ (2006) *J Exp Biol* 209:260–272.
19. Gao HJ, Wang X, Yao HM, Gorb S, Arzt E (2005) *Mech Mater* 37:275–285.
20. Huber G, Gorb S, Spolenak R, Arzt E (2005) *Biol Lett* 1:2–4.
21. Kendall K (1975) *J Phys D* 8:1449–1452.
22. Ciccotti M, Giorgini B, Vallet D, Barquins M (2004) *Int J Adhes Adhes* 24:143–151.
23. Israelachvili J (1992) *Intermolecular and Surface Forces* (Academic, New York).
24. Autumn K, Ryan MJ, Wake DB (2002) *Q Rev Biol* 77:383–408.
25. Arzt E, Gorb S, Spolenak R (2003) *Proc Natl Acad Sci USA* 100:10603–10606.
26. Autumn K (2006) in *Biological Adhesives*, eds Smith A, Callow J (Springer, Berlin), pp 225–255.
27. Autumn K, Hsieh ST, Dudek DM, Chen J, Chitaphan C, Full RJ (2006) *J Exp Biol* 209:260–272.
28. Chen JJ, Peattie AM, Autumn K, Full RJ (2006) *J Exp Biol* 209:249–259.
29. Israelachvili J, Maeda N, Rosenberg KJ, Akbulut M (2005) *J Mater Res* 20:1952–1972.
30. Urbakh M, Klafter J, Gourdon D, Israelachvili J (2004) *Nature* 430:525–528.
31. Bowden FP, Tabor D (1950) *Friction and Lubrication of Solids* (Clarendon, Oxford).
32. He G, Muser MH, Robbins MO (1999) *Science* 284:1650–1652.